Inorganic Chemistry

Article

pubs.acs.org/IC

Intramolecular d^{10}–d^{10} Interactions in a $Ni_6C(CO)_9(AuPPh_3)_4$ Bimetallic Nickel–Gold Carbide Carbonyl Cluster

Iacopo Ciabatti,[†] Cristina Femoni,[†] Maria Carmela Iapalucci,[†] Andrea Ienco,[‡] Giuliano Longoni,[†] Gabriele Manca,[‡] and Stefano Zacchini*[,†]

[†]Dipartimento di Chimica Industriale "Toso Montanari", Università di Bologna, Viale Risorgimento 4, 40136 Bologna, Italy

[‡]Consiglio Nazionale delle Ricerche, Istituto di Chimica dei Composti Organo Metallici, Via Madonna del Piano 10, 50019 Sesto Fiorentino, Florence, Italy

Supporting Information

ABSTRACT: The $Ni_6C(CO)_9(AuPPh_3)_4$ bimetallic carbide carbonyl cluster was obtained from the reaction of $[Ni_9C(CO)_{17}]^{2-}$ with $Au(PPh_3)Cl$. It contains a rare carbon-centered (distorted) Ni_6C octahedral core decorated by four $Au(PPh_3)$ fragments. These are μ_3-bonded to four contiguous Ni_3-triangular faces and display weak intramolecular Au···Au d^{10}–d^{10} interactions. The cluster has been characterized in the solid state on two different solvato crystals, i.e., $Ni_6C(CO)_9(AuPPh_3)_4\cdot THF$ and $Ni_6C(CO)_9(AuPPh_3)_4\cdot THF\cdot 0.5C_6H_{14}$. The two solvates show some interesting differences concerning the weak Au···Au contacts. Density functional theory calculations have demonstrated that the presence of the two isomers is related to solid-state packing effects and not to the existence of two double minima in the potential energy surface. This, in turn, confirms that Au···Au d^{10}–d^{10} interactions are rather soft and thus influenced also by weak van der Waals forces because of the interaction of the cluster with the cocrystallized solvent molecules.

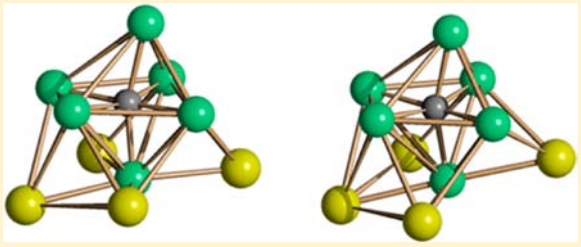

1. INTRODUCTION

Weak d^{10}–d^{10} metal–metal interactions are now widely documented in the chemistry of gold(I) complexes and clusters, and the term "aurophilicity" is commonly used to refer to such interactions.[1−4] Although positively charged Au^I ions could be expected to repel each other on the basis of electrostatics, the attractive interactions between these closed-valence-shell ions result in interatomic distances typically in the range between 2.7 and 3.3 Å, often shorter than the sum of the van der Waals radii.[1−4] This phenomenon could not be explained by conventional descriptions of chemical bonding but is now well described as dispersion-driven and enhanced by relativistic effects.[1−5] However, the conditions for the occurrence of aurophilicity and its structural, physical, and chemical consequences remain difficult to predict; hence, further experimental and theoretical studies on d^{10}–d^{10} interactions are needed, whether in homo- or in heterometallic systems.[1−6]

Some interesting examples of aurophilic interactions are documented also for metal carbonyl clusters containing two or more $[AuPPh_3]^+$ fragments.[3b,7] On the basis of the isolobal analogy between $[AuPPh_3]^+$ and H^+,[8,9] the former has been widely employed in metal carbonyl cluster chemistry in order to get structural information on the location of hydrides. Nonetheless, the occurrence of aurophilic interactions often invalidates these considerations when two or more Au^I ions are present. For instance, intramolecular $Au^I\cdots Au^I$ interactions cause structural differences between $Fe_3S(CO)_9(AuPPh_3)_2$ and $H_2Fe_3S(CO)_9$.[10]

The M_6C octahedral framework present in several monocarbide carbonyl clusters seems to be an interesting platform to test aurophilicity.[11−15] In these clusters, the $[AuPPh_3]^+$ fragment might be coordinated to an edge or a face of the octahedron. Moreover, when a second fragment is added, several options arise because it can coordinate to a site close or far from the first one. Aurophilicity favors the proximity of the two Au^I centers and the formation of intramolecular d^{10}–d^{10} interactions, as exemplified in $Rh_6C(CO)_{13}(AuPPh_3)_2$ and $Co_6C(CO)_{13}(AuPPh_3)_2$.[16,17]

It was, thus, of interest to investigate analogous octahedral M_6C carbonyl clusters containing more than two $[AuPPh_3]^+$ fragments, in order to see whether more extended Au···Au interactions were formed and to evaluate the importance of such interactions in larger clusters. Herein, we report the synthesis and structural characterization of the neutral $Ni_6C(CO)_9(AuPPh_3)_4$ cluster, which contains four of these fragments. Its structure has been determined on two different solvate crystals, i.e., $Ni_6C(CO)_9(AuPPh_3)_4\cdot THF$ and $Ni_6C(CO)_9(AuPPh_3)_4\cdot THF\cdot 0.5C_6H_{14}$ (THF = tetrahydrofuran), showing some interesting differences regarding the weak Au···Au contacts. Density functional theory (DFT) calculations have been performed in order to establish whether the presence of two isomers is related to solid-state packing effects or the existence of two double minima in the potential energy surface. In addition, $Ni_6C(CO)_9(AuPPh_3)_4$ represents the first example

Received: June 18, 2013
Published: September 5, 2013

   dx.doi.org/10.1021/ic401540s | Inorg. Chem. 2013, 52, 10559−10565

of an octahedral monocarbidonickel carbonyl cluster. Thus, the octahedral M_6C framework is very common for carbonyl clusters of group 8 and 9 metals, whereas up to now, it was completely unknown for carbonyls of group 10 metals.[11−15]

2. RESULTS AND DISCUSSION

2.1. Synthesis of $Ni_6C(CO)_9(AuPPh_3)_4$. The neutral cluster $Ni_6C(CO)_9(AuPPh_3)_4$ was obtained in low yield from the reaction of $[Ni_9C(CO)_{17}]^{2-}$[18] with $Au(PPh_3)Cl$ (ca. 2 equiv) in THF. The formation of $Ni_6C(CO)_9(AuPPh_3)_4$ is accompanied by several byproducts, such as $Ni(CO)_4$, Ni^{2+}, $Ni(CO)_3(PPh_3)$, $[Ni_8C(CO)_{16}]^{2-}$, gold metal, and unreacted $[Ni_9C(CO)_{17}]^{2-}$. All of the carbonyl byproducts [i.e., $Ni(CO)_4$, $Ni(CO)_3(PPh_3)$, $[Ni_8C(CO)_{16}]^{2-}$, $[Ni_9C(CO)_{17}]^{2-}$] have been identified through IR spectroscopy by comparison with the spectra reported in the literature. The presence of Ni^{2+} salts was confirmed by the typical green color of the water solution used to wash the residue (see below) and confirmed using dimethylglyoxime. The formation of gold metal was confirmed by the typical gold mirror.

Purification was accomplished by removal of the solvent in vacuo and washing of the residue with water (to remove Ni^{II} salts) and toluene (to remove neutral mononuclear species). The residue was then extracted in THF and recrystallized from THF/toluene and THF/*n*-hexane, resulting in X-ray-quality crystals of $Ni_6C(CO)_9(AuPPh_3)_4\cdot THF$ and $Ni_6C(CO)_9(AuPPh_3)_4\cdot THF\cdot 0.5C_6H_{14}$, respectively. Under these conditions, anionic species such as $[Ni_8C(CO)_{16}]^{2-}$ and $[Ni_9C(CO)_{17}]^{2-}$ preferentially remained in solution or precipitated as amorphous solids. Crystals for X-ray analyses were, therefore, mechanically separated from the amorphous material before proceeding further with analysis. The crystals show ν(CO) in a Nujol mull at 2027(ms), 1984(vs), 1970(s), 1851(m), and 1832(ms) cm^{-1}. These crystals are almost insoluble in all organic solvents, hampering any further chemical, spectroscopic, or physical study.

2.2. Crystal Structures of $Ni_6C(CO)_9(AuPPh_3)_4\cdot THF$ and $Ni_6C(CO)_9(AuPPh_3)_4\cdot THF\cdot 0.5C_6H_{14}$. The structure of the neutral cluster $Ni_6C(CO)_9(AuPPh_3)_4$ has been determined on two different solvato solids, i.e., $Ni_6C(CO)_9(AuPPh_3)_4\cdot THF$ and $Ni_6C(CO)_9(AuPPh_3)_4\cdot THF\cdot 0.5C_6H_{14}$. The cluster displays a similar structure in both solvates, even if there are some differences especially regarding the weak Au···Au contacts. The molecular structure of the cluster, as found in the two solvates, is represented in Figure 1, whereas the most relevant bond lengths are compared in Table 1.

The $Ni_6C(CO)_9(AuPPh_3)_4$ cluster contains a carbon-centered distorted Ni_6C octahedral core (Figure 2). The four $Au(PPh_3)$ fragments are μ_3-bonded to four contiguous triangular faces (related by 4-fold) of the octahedron, formally reducing the symmetry from O_h to C_{4v}. Actually, the cluster displays C_1 symmetry in view of its heavy distortions. For what concerns the nine CO ligands, six are terminally coordinated one per each Ni atom, whereas the remaining three carbonyls are edge bridging, one in the equatorial plane of the cluster and the other two on two edges spanning from the equatorial plane toward the apical Ni atom nonbonded to any Au atom.

The four Ni atoms in the equatorial plane of the cluster as well as the carbide atom are almost coplanar [mean deviation from the least-squares plane 0.0551 and 0.0466 Å for the two solvates, respectively], whereas the other two Ni atoms are in apical positions [Ni_{ap}−C−Ni_{ap} 163.6(4) and 159.7(6)°], one bonded to four Au atoms and the other to none. The cluster may be partitioned into an anionic $[Ni_6C(CO)_9]^{4-}$ moiety decorated by four cationic $[AuPPh_3]^+$ units.

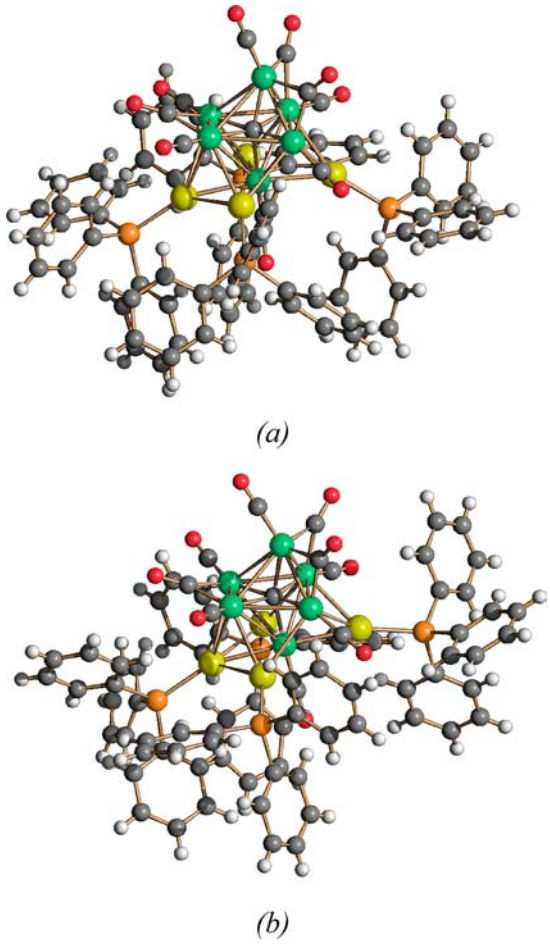

Figure 1. Molecular structure of $Ni_6C(CO)_9(AuPPh_3)_4$ as found in $Ni_6C(CO)_9(AuPPh_3)_4\cdot THF$ (a) and $Ni_6C(CO)_9(AuPPh_3)_4\cdot THF\cdot 0.5C_6H_{14}$ (b). Color code: green, Ni; yellow, Au; orange, P; gray, C; white, H.

Table 1. Comparison of the Most Relevant Bond Lengths (Å) in $Ni_6C(CO)_9(AuPPh_3)_4\cdot THF$ and $Ni_6C(CO)_9(AuPPh_3)_4\cdot THF\cdot 0.5C_6H_{14}$

	$Ni_6C(CO)_9(AuPPh_3)_4\cdot THF$	$Ni_6C(CO)_9(AuPPh_3)_4\cdot THF\cdot 0.5C_6H_{14}$
Ni−Ni	2.3891(12)−2.8687(12)	2.3847(18)−2.9875(18)
	average 2.678(4)	average 2.682(6)
Ni−$C_{carbide}$[a]	1.811(6)−1.931(6)	1.816(9)−1.920(9)
	average 1.893(16)	average 1.89(2)
Ni−Au	2.5625(8)−2.9323(9)	2.5738(12)−2.8615(14)
	average 2.696(3)	average 2.702(5)
Au−P	2.2836(19)-2.2914(19)	2.287(3)-2.298(3)
	average 2.289(4)	average 2.294(6)
Au···Au[b]	3.5922(5), 3.0509(5), 4.2721(5), 3.6648(5)	3.1701(7), 2.9889(7), 4.3230(7), 4.0611(7)
	average 3.6450(10)	average 3.6358(14)

[a] $C_{carbide}$ refers to the interstitial carbide atom. [b] All contacts (bonding and nonbonding) have been considered.

The Ni−Ni contacts are rather spread [2.3891(12)−2.8687(12) Å, average 2.678(4) Å for $Ni_6C(CO)_9(AuPPh_3)_4\cdot THF$; 2.3847(18)−2.9875(18) Å, average 2.682(6) Å for

dx.doi.org/10.1021/ic401540s | Inorg. Chem. 2013, 52, 10559−10565

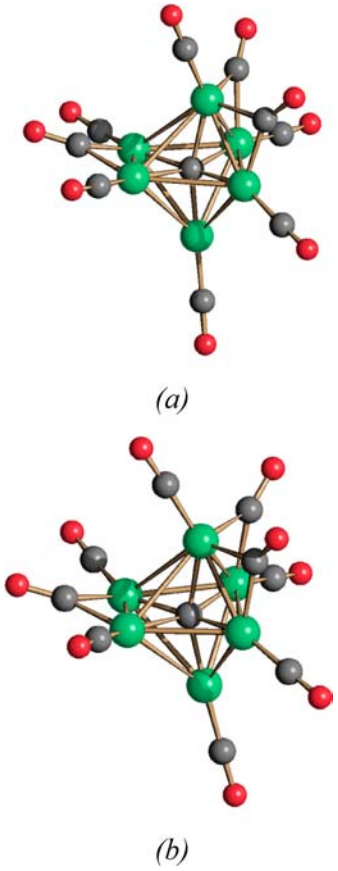

Figure 2. $Ni_6C(CO)_9$ core of $Ni_6C(CO)_9(AuPPh_3)_4$ as found in $Ni_6C(CO)_9(AuPPh_3)_4$·THF (a) and $Ni_6C(CO)_9(AuPPh_3)_4$·THF·$0.5C_6H_{14}$ (b). Color code: green, Ni; gray, C.

$Ni_6C(CO)_9(AuPPh_3)_4$·THF·$0.5C_6H_{14}$] and may be divided into three sets: (a) four Ni–Ni contacts in the equatorial plane [2.3891(12)–2.8687(12) Å, average 2.682(2) Å; 2.3847(18)–2.9875(18) Å, average 2.685(4) Å], (b) four Ni–Ni contacts from the equatorial plane toward the apical Ni atom nonbonded to any Au atom [2.4521(11)–2.8989(12) Å, average 2.644(2) Å; 2.4616(18)–2.8492(17) Å, average 2.635(4)Å], and (c) four Ni–Ni contacts capped by the four $Au(PPh_3)$ fragments [2.5830(12)–2.7918(11) Å, average 2.707(2) Å; 2.5371(17)–2.8817(17) Å, average 2.726(4) Å]. The resulting octahedral cages are very distorted, with the 12 Ni–Ni edges very different, in virtue of the fact that the interstitial carbide atom is rather big to be accommodated in a regular octahedron.

$Ni_6C(CO)_9(AuPPh_3)_4$ represents a very rare case of a nickel cluster containing a carbide atom within an octahedral cage and the first case for monocarbidonickel carbonyl clusters. As far as we are aware, the only monocarbide species displaying a (heavily distorted) octahedrally coordinated carbide is the cyclopentadienyl cluster $Ni_6C(Cp)_6$.[19] Focusing our attention on carbonyl clusters, all nickel monocarbides reported to date displayed larger cages, such as trigonal-prismatic or square-antiprismatic, i.e., $[Ni_7C(CO)_{12}]^{2-}$, $[Ni_8C(CO)_{16}]^{2-}$, $[Ni_9C(CO)_{17}]^{2-}$, and $[Ni_{10}C(CO)_{18}]^{2-}$.[18,20] Only in the case of the octacarbides $[Ni_{36}C_8(CO)_{36}(Cd_2Cl_3)]^{5-}$ and $[Ni_{36-y}C_8(CO)_{34-y}(MeCN)_3(Cd_2Cl_3)]^{3-}$ [21] were four of the eight carbide atoms contained within distorted octahedral cages, whereas the other four carbides were located in two trigonal-prismatic and two monocapped trigonal-prismatic cages. The Ni–$C_{carbide}$ contacts in $Ni_6C(CO)_9(AuPPh_3)_4$ [1.811(6)–1.931(6) Å, average 1.893(16) Å, and 1.816(9)–1.920(9) Å, average 1.89(2) Å, for the two solvates, respectively] compare very well to the octahedral cages of $[Ni_{36}C_8(CO)_{36}(Cd_2Cl_3)]^{5-}$ and $[Ni_{36-y}C_8(CO)_{34-y}(MeCN)_3(Cd_2Cl_3)]^{3-}$ [1.874(8)–1.956(8) Å, average 1.90 Å, and 1.865(7)–2.003(8) Å, average 1.90 Å, respectively], whereas the Ni–$C_{carbide}$ contacts in $Ni_6C(Cp)_6$[19] are more scattered [1.767(4)–2.109(4) Å, average 1.897(9) Å].

Each Au atom is tetracoordinated to a Ni_3 face of the octahedron and a PPh_3 ligand. The Ni–Au contacts [2.5625(8)–2.9323(9) Å, average 2.696(3) Å; 2.5738(12)–2.8615(14) Å, average 2.702(5) Å] are rather spread but in keeping with those previously reported for other nickel–gold carbonyl clusters such as $[Ni_{12}Au(CO)_{24}]^{3-}$, $[Ni_{32}Au_6(CO)_{44}]^{6-}$, and $[Ni_{12}Au_6(CO)_{24}]^{6-}$.[22,23]

Four Au···Au contacts are present in the cluster, displaying similar average values in the two solvates [3.6450(10) and 3.6358(14) Å, respectively] but distributed in a rather different manner (Figure 3). Thus, in $Ni_6C(CO)_9(AuPPh_3)_4$·THF, only

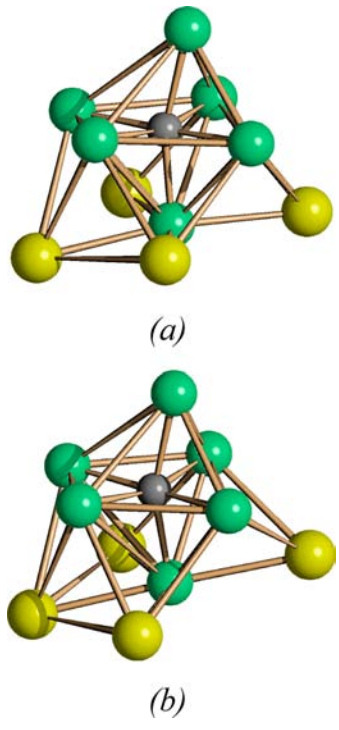

Figure 3. Ni_6CAu_4 core of $Ni_6C(CO)_9(AuPPh_3)_4$ as found in $Ni_6C(CO)_9(AuPPh_3)_4$·THF (a) and $Ni_6C(CO)_9(AuPPh_3)_4$·THF·$0.5C_6H_{14}$ (b).

one contact may be considered at bonding distance [3.0509(5) Å], whereas the other three contacts [3.5922(5), 3.6648(5), and 4.2721(5) Å] are well above the sum of the van der Waals radii of gold [sum of the covalent radii 2.72 Å; sum of the van der Waals radii 3.32 Å].[24] Conversely, in $Ni_6C(CO)_9(AuPPh_3)_4$·THF·$0.5C_6H_{14}$, two contiguous Au···Au contacts are at bonding distances [2.9889(7) and 3.1701(7) Å], whereas the other two are nonbonding [4.0611(7) and 4.3230(7) Å].

Interestingly, the four Au atoms as well as the apical Ni atom bonded to them lie in the same plane in $Ni_6C(CO)_9(AuPPh_3)_4$·THF·$0.5C_6H_{14}$ [mean deviation from the least-squares plane 0.0219 Å], whereas they significantly deviate from the common

dx.doi.org/10.1021/ic401540s | Inorg. Chem. 2013, 52, 10559–10565

plane in $Ni_6C(CO)_9(AuPPh_3)_4$·THF [mean deviation from the least-squares plane 0.1059 Å]. Moreover, these planes form rather different angles with the equatorial plane [the one comprising the four equatorial Ni atoms and the carbide] in $Ni_6C(CO)_9(AuPPh_3)_4$·THF [6.6°] compared to $Ni_6C(CO)_9(AuPPh_3)_4$·THF·0.5C_6H_{14} [11.0°].

2.3. Theoretical Investigation. In order to better understand the factors that rule such a dichotomy found in the solid state, a theoretical investigation was performed at the B3LYP-DFT/6-31+G(d,p) level of theory with the Stuttgart–Dresden *pseudo*potential for both Au and Ni centers. Two simplified models were built from the X-ray structures upon substitution of the bulky PPh_3 with the simpler PH_3 and by neglect of the cocrystallized solvent molecule. Single-point-energy calculations on the structure models revealed that the structure found in $Ni_6C(CO)_9(AuPPh_3)_4$·THF·0.5C_6H_{14} is more stable by 4.95 kcal mol^{-1} than the one present in $Ni_6C(CO)_9(AuPPh_3)_4$·THF. This difference in stability is consistent either with a solid-state packing effect or with weak Au–Au interactions. Optimization of both of these models converged to the same structure with an angle Ni_{ap}–C–Ni_{ap} of 159.5° and very similar to the one found in $Ni_6C(CO)_9(AuPPh_3)_4$·THF·0.5C_6H_{14} (see Figure 4 and Table 2). This suggests that the more stable geometry is the one found in $Ni_6C(CO)_9(AuPPh_3)_4$·THF·0.5C_6H_{14}, with two short and two long Au···Au distances. Conversely, the one present in $Ni_6C(CO)_9(AuPPh_3)_4$·THF with a single short Au···Au contact is less stable (by ca. 5 kcal mol^{-1}). The presence in the solid state of this structure may be justified by assuming that packing effects compensate for its minor stability as an isolated molecule.

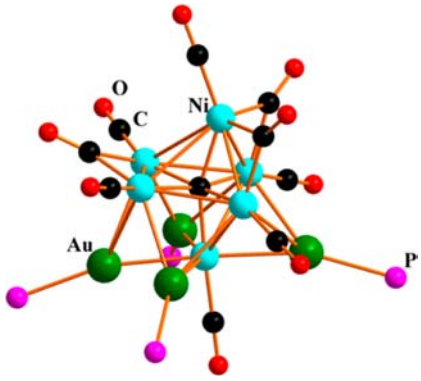

Figure 4. Optimized structure of $Ni_6C(CO)_9(AuPPh_3)_4$ at the B3LYP-DFT level of theory.

In the optimized structure, the Ni–Ni contacts spread over a large range (2.39–3.04 Å), and they can be divided into three different sets: the in-plane ones (2.42–3.04 Å), Ni_{ap}–Ni_{eq} not involved in interactions with Au centers (2.39–2.80 Å), and the one in the gold-capping half (2.59–2.92 Å). The calculated Ni–$C_{carbide}$ distances are 1.93 Å with the only exception of the one between the apical Ni atoms, interacting with the Au atoms (1.83 Å). Although there is some overestimation by the calculations, likely imputed to the usage of a *pseudo*potential for the metal atoms and a simplified model, the computed structure satisfactorily reproduces the Ni_6C core. Interestingly, the four capping Au atoms and the apical Ni atom lie all in the same plane as $Ni_6C(CO)_9(AuPPh_3)_4$·THF·0.5C_6H_{14}. The Au··· Au distances are in pairs: two short (3.14 Å) and two long (4.22 Å), quite resembling the structure of $Ni_6C(CO)_9(AuPPh_3)_4$·THF·0.5C_6H_{14}.

The highest occupied molecular orbital (HOMO)–lowest unoccupied molecular orbital (LUMO) gap was estimated to be 2.54 eV. The HOMO (Figure 5a) is calculated to be mainly localized on the Ni_6 core; in contrast, the LUMO (Figure 5b) has a strong contribution from the Au and apical Ni centers. The main contributions to metal bonding come from the interaction between fully occupied d orbital combinations of the Ni atoms with the empty sp hybrids on the Au centers.

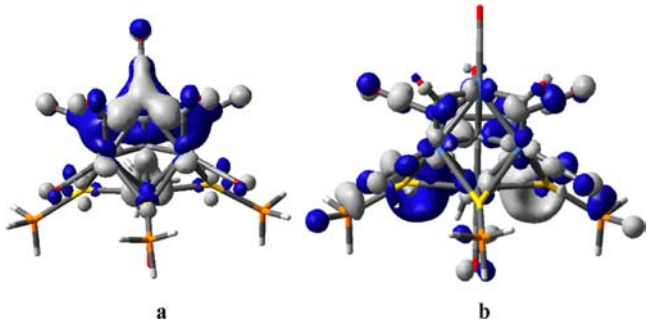

Figure 5. Graphical plots of the (a) HOMO and (b) LUMO orbitals of $Ni_6C(CO)_9(Au(PH_3)_4$.

In principle, a functional with inclusion of the dispersion forces as B97D could help to reproduce the two isomers in the case that structural differences between the two experimental

Table 2. Experimental and Calculated Bond Lengths (Å) and Angles (deg) of $Ni_6C(CO)_9(AuPPh_3)_4$

	$Ni_6C(CO)_9(AuPPh_3)_4$·THF	$Ni_6C(CO)_9(AuPPh_3)_4$·THF·0.5C_6H_{14}	calcd B3LYP-DFT/6-31+G(d,p)
Ni_{eq}–Ni_{eq}	2.3891(12)–2.8687(12)	2.3847(18)–2.9875(18)	2.42–3.04
Ni_{eq}–Ni_{ap} (no-Au)	2.4521(11)–2.8989(12)	2.4616(18)–2.8492(17)	2.39–2.80
Ni_{eq}–Ni_{ap} (Au)	2.5830(12)–2.7918(11)	2.5371(17)–2.8817(17)	2.59–2.92
$C_{carbide}$–Ni_{eq}	1.880(6)–1.920(7)	1.901(10)–1.919(9)	1.93
$C_{carbide}$–Ni_{ap} (no Au)	1.931(6)	1.920(9)	1.93
$C_{carbide}$–Ni_{ap} (Au)	1.811(6)	1.816(9)	1.83
Ni–Au	2.5625(8)–2.9323(9)	2.5738(12)–2.8615(14)	2.60–2.87
Au–P	2.2836(19)–2.2914(19)	2.287(3)–2.298(3)	2.38–2.40
Au···Au	3.5922(5)	3.1701(7)	3.14
	3.0509(5)	2.9889(7)	3.14
	4.2721(5)	4.3230(7)	4.22
	3.6648(5)	4.0611(7)	4.22
Ni_{ap}–C–Ni_{ap}	163.6(4)	159.7(6)	159.5

dx.doi.org/10.1021/ic401540s | *Inorg. Chem.* 2013, 52, 10559–10565

structures are given by variable Au···Au interactions. As occurred for the B3LYP functional, the calculations converged into the same structure with quite short Au···Au distances between 3.59 and 3.85 Å. Although there are some slight differences in the obtained Ni−Ni distances, especially for those involving the Ni atom bonded to Au atoms, the other main features remain quite unaltered. The HOMO−LUMO gap calculated with the B97D functional was 1.58 eV. Because also inclusion of the dispersion corrections is not able to reproduce the double minimum features of the potential energy surface, such behavior could be reasonably imputed to solid-state packing in the crystal because of weak interaction with the cocrystallized solvent molecules.

The experimental IR spectrum in a Nujol mull displays five main peaks at 2027, 1984, 1970, 1851, and 1832 cm^{-1}, respectively. Through frequency calculations, performed within the *Gaussian 09* package on the optimized geometries, we attempted assignment of the different carbonyl stretchings (Table 3). In fact, although slightly different in position (2114, 2062, 2038, 1972, and 1935 cm^{-1}) and sometimes derived from a complex vibrational pattern, they can be simply attributed to the different carbonyl moieties. The first three peaks could be assigned to the terminal CO: the high-energy one to CO bonded to the apical Ni atom without interaction with the Au centers, the second to the in-plane ones, and the last to the remaining apical one. The calculated stretchings of the bridging CO ligands occur at 1935 and 1970 cm^{-1} respectively for the in-plane and out-of-plane carbonyl ligands.

Table 3. Experimental and Calculated ν(CO) Stretchings (cm^{-1}) of $Ni_6C(CO)_9(AuPPh_3)_4$

assignment	multiplicity	experimental (Nujol mull)	calculated
t-CO Ni_{ap} (no Au)	1	2027(ms)	2114
t-CO Ni_{eq}	4	1984(vs)	2062
t-CO Ni_{ap} (Au)	1	1970(s)	2038
μ-CO Ni_{eq}	1	1851(m)	1972
μ-CO Ni_{ap}	2	1832(ms)	1935

3. CONCLUSIONS

A new bimetallic $Ni_6C(CO)_9(AuPPh_3)_4$ monocarbide cluster has been synthesized and structurally characterized. It may be viewed as composed of an octahedral $[Ni_6C(CO)_9]^{4-}$ core capped by four $[AuPPh_3]^+$ fragments. It represents the first example of an octahedral monocarbidonickel carbonyl cluster because, due to steric effects, C atoms are usually lodged into larger cavities in nickel monocarbide clusters, i.e., trigonal-prismatic or square-antiprismatic.[18,20] This results in heavy distortion of the octahedral geometry, as was recently found in the (heavy distorted) octahedral $Ni_6C(Cp)_6$cyclopentadienyl monocarbide cluster.[19]

The $[Ni_6C(CO)_9]^{4-}$ core of $Ni_6C(CO)_9(AuPPh_3)_4$ possesses 86 cluster valence electrons (CVEs), as expected for an octahedral cluster.[25,26] Conversely, $Ni_6C(Cp)_6$ is considerably electron-richer and displays 94 CVEs. This increase in CVEs results in the opening of the octahedral cage of $Ni_6C(Cp)_6$ by breaking two Ni−Ni edges.[19] Conversely, in the case of $Ni_6C(CO)_9(AuPPh_3)_4$, even if the Ni_6C octahedron is rather distorted, the 12 Ni−Ni contacts are all at bonding distances, in keeping with its electron count.

The structure of $Ni_6C(CO)_9(AuPPh_3)_4$ has been determined in two different solvate salts, which mainly differ in the distribution of the four Au···Au contacts. DFT calculations clearly point out that these deformations arise from packing effects due to van der Waals interactions of the neutral clusters with the cocrystallized solvent molecules. The fact that the Au atoms are the ones more affected by these weak forces confirms that Au···Au d^{10}−d^{10} interactions are rather soft and, thus, influenced also by weak forces. Finally, the present work demonstrates that the M_6C octahedral framework present in some monocarbide carbonyl clusters may be an interesting platform to test aurophilicity.

4. EXPERIMENTAL SECTION

4.1. General Procedures. All reactions and sample manipulations were carried out using standard Schlenk techniques under nitrogen and in dried solvents. All of the reagents are commercial products (Aldrich) of the highest purity available and were used as received, except $[NEt_4]_2[Ni_9C(CO)_{17}]$[18] and $Au(PPh_3)Cl$[26], which have been prepared according to the literature. Analyses of nickel and gold were performed by atomic absorption on a Pye-Unicam instrument. Analyses of carbon, hydrogen, and nitrogen were obtained with a ThermoQuestFlashEA 1112NC instrument. IR spectra were recorded on a Perkin-Elmer SpectrumOne interferometer in CaF_2 cells. Structure drawings have been performed with *SCHAKAL99*.[27]

4.2. Synthesis of $Ni_6C(CO)_9(AuPPh_3)_4$·THF. $Au(PPh_3)Cl$ (0.52 g, 1.04 mmol) was added in solid to a solution of $[NEt_4]_2[Ni_9C(CO)_{17}]$ (0.664 g, 0.520 mmol) in THF (30 mL) over a period of 2 h. The resulting mixture was further stirred at room temperature for 6 h and then the solvent removed in vacuo. The residue was washed with water (40 mL) and toluene (40 mL), dried in vacuo, and extracted with THF (20 mL). Crystals of $Ni_6C(CO)_9(AuPPh_3)_4$·THF suitable for X-ray analysis were obtained after layering toluene (40 mL) on the THF solution (yield 0.24 g, 12% based on nickel).

Anal. Calcd for $C_{86}H_{68}Au_4Ni_6O_{10}P_4$ (2525.41): C, 40.90; H, 2.71; Au, 31.20; Ni, 13.94. Found: C, 40.71; H, 2.94; Au, 31.35; Ni, 14.09. IR (Nujol, 293 K): ν(CO) 2027(ms), 1984(vs), 1970(s), 1851(m), 1832(ms) cm^{-1}.

4.3. Synthesis of $Ni_6C(CO)_9(AuPPh_3)_4$·THF·0.5C_6H_{14}. $Au(PPh_3)Cl$ (0.57 g, 1.15 mmol) was added in solid to a solution of $[NEt_4]_2[Ni_9C(CO)_{17}]$ (0.730 g, 0.572 mmol) in THF (30 mL) over a period of 2 h. The resulting mixture was further stirred at room temperature for 6 h and then the solvent removed in vacuo. The residue was washed with water (40 mL) and toluene (40 mL), dried in vacuo, and extracted with THF (20 mL). Crystals of $Ni_6C(CO)_9(AuPPh_3)_4$·THF·0.5C_6H_{14} suitable for X-ray analysis were obtained after layering *n*-hexane (40 mL) on the THF solution (yield 0.22 g, 10% based on nickel).

Anal. Calcd for $C_{89}H_{74}Au_4Ni_6O_{10}P_4$ (2567.49): C, 41.64; H, 2.91; Au, 30.69; Ni, 13.72. Found: C, 41.51; H, 3.02; Au, 30.81; Ni, 13.64. IR (Nujol, 293 K): ν(CO) 2027(ms), 1984(vs), 1970(s), 1851(m), 1832(ms) cm^{-1}.

4.4. X-ray Crystallographic Study. Crystal data and collection details for $Ni_6C(CO)_9(AuPPh_3)_4$·THF and $Ni_6C(CO)_9(AuPPh_3)_4$·THF·0.5C_6H_{14} are reported in Table 4. The diffraction experiments were carried out on a Bruker APEX II diffractometer equipped with a CCD detector using Mo Kα radiation. Data were corrected for Lorentz polarization and absorption effects (empirical absorption correction *SADABS*).[28] Structures were solved by direct methods and refined by full-matrix least squares based on all data using F^2.[29] H atoms were fixed at calculated positions and refined by a riding model. All non-H atoms in the cluster molecules were refined with anisotropic displacement parameters, whereas solvent molecules were treated isotropically.

$Ni_6C(CO)_9(AuPPh_3)_4$·THF. The asymmetric unit of the unit cell contains one cluster and one THF molecule (all located on general positions). Similar *U* restraints (s.u. 0.01) were applied to the C and O atoms. Two CO ligands in the cluster are disordered and, therefore, they have been split into two positions each and refined with one occupancy factor per disordered group. Restraints to bond distances

dx.doi.org/10.1021/ic401540s | *Inorg. Chem.* 2013, 52, 10559−10565

Table 4. Crystal Data and Experimental Details for $Ni_6C(CO)_9(AuPPh_3)_4$·THF and $Ni_6C(CO)_9(AuPPh_3)_4$·THF·$0.5C_6H_{14}$

	$Ni_6C(CO)_9(AuPPh_3)_4$·THF	$Ni_6C(CO)_9(AuPPh_3)_4$·THF·$0.5C_6H_{14}$
formula	$C_{86}H_{68}Au_4Ni_6O_{10}P_4$	$C_{89}H_{74}Au_4Ni_6O_{10}P_4$
fw	2525.41	2567.49
T, K	293(2)	295(2)
λ, Å	0.71073	0.71073
cryst syst	monoclinic	monoclinic
space group	$P2_1/n$	$P2_1/n$
a, Å	15.4746(9)	15.493(2)
b, Å	24.3295(14)	22.922(4)
c, Å	22.3941(13)	24.490(4)
β, deg	91.8920(10)	90.978(2)
cell volume, Å^3	8426.5(8)	8696(2)
Z	4	4
D_c, g cm^{-3}	1.991	1.961
μ, mm^{-1}	8.374	8.117
$F(000)$	4832	4928
cryst size, mm^3	0.16 × 0.13 × 0.10	0.18 × 0.16 × 0.12
θ limits, deg	1.24−25.03	1.54−25.03
index ranges	$-18 \le h \le 18$, $-28 \le k \le 28$, $-26 \le l \le 26$	$-18 \le h \le 18$, $-27 \le k \le 27$, $-29 \le l \le 29$
reflns collected	80483	82307
indep reflns	14881 (R_{int} = 0.0542)	15347 (R_{int} = 0.0915)
completeness to θ_{max}, %	100.0	99.9
data/restraints/param	14881/574/1004	15347/514/990
GOF on F^2	1.007	1.005
R1 [$I > 2\sigma(I)$]	0.0340	0.0451
wR2 (all data)	0.0804	0.1173
largest diff peak/hole, e Å^{-3}	1.103/−0.609	2.952/−1.324

were applied as follows (s.u. 0.02): 1.43 Å for C−O and 1.53 Å for C−C in THF.

$Ni_6C(CO)_9(AuPPh_3)_4$·THF·$0.5C_6H_{14}$. The asymmetric unit of the unit cell contains one cluster, one THF molecule (all located on general positions), and half of a C_6H_{14} molecule (on a 2 axis). The latter is disordered over two symmetry-related positions and has been refined isotropically with 0.5 occupancy factor. Similar U restraints (s.u. 0.005) were applied to the C and O atoms. The O atoms of the CO ligands have been restrained to isotropic behavior (ISOR line in *SHELXL*; s.u. 0.01). Restraints to bond distances were applied as follows (s.u. 0.02): 1.43 Å for C−O and 1.53 Å for C−C in THF; 1.53 Å for C−C in C_6H_{14}.

4.5. Computational Details. The models were optimized at the hybrid DFT using B3LYP[30] and B97D[31] functionals within the *Gaussian 09* program.[32] For all of the fully optimized structures, calculations of the vibrational frequencies were performed to confirm their nature as stationary points. The effective Stuttgart−Dresden core potential[33] was adopted for the Au and Ni atoms, while for the remaining atomic species, the basis set used was 6-31G, with the important addition of the polarization functions (d and p) for all s, including the H atoms. The coordinates of the optimized structure have been reported in the Supporting Information.

■ ASSOCIATED CONTENT

Ⓢ Supporting Information

CIF files giving X-ray crystallographic data for the structure determination of $Ni_6C(CO)_9(AuPPh_3)_4$·THF and $Ni_6C(CO)_9(AuPPh_3)_4$·THF·$0.5C_6H_{14}$ and Cartesian coordinates of the optimized structure of $Ni_6C(CO)_9(AuPH_3)_4$. This material is available free of charge via the Internet at http://pubs.acs.org.

■ AUTHOR INFORMATION

Corresponding Author

*E-mail: stefano.zacchini@unibo.it. Fax: +39 0512093690.

Notes

The authors declare no competing financial interest.

■ ACKNOWLEDGMENTS

Financial support of Università di Bologna is gratefully acknowledged. Funding by Fondazione CARIPLO (Project 2011-0289) is heartily acknowledged. A.I. and G.M. acknowledge ISCRA-CINECA HP Grant HP10BNL89W for computational resources.

■ REFERENCES

(1) (a) Schmidbaur, H.; Schier, A. *Chem. Soc. Rev.* **2012**, *41*, 370. (b) Chen, Z. N.; Zhao, N.; Fan, Y.; Ni, J. *Coord. Chem. Rev.* **2009**, *253*, 1. (c) Laguna, A. *Modern supramolecular gold chemistry: gold−metal interactions and applications*; Wiley-VCH: Weinheim, Germany, 2008. (d) Pyykkö, P. *Chem. Rev.* **1997**, *97*, 597.

(2) (a) Schmidbaur, H.; Schier, A. *Chem. Soc. Rev.* **2008**, *37*, 1932. (b) Katz, M. J.; Sakaib, K.; Leznoff, D. B. *Chem. Soc. Rev.* **2008**, *37*, 1884. (c) Schmidbaur, H. *Gold Bull.* **2000**, *33*, 3. (d) Kim, P.-S. G.; Hu, Y.; Brandys, M.-C.; Burchell, T. J.; Puddephatt, R. J.; Sham, T. K. *Inorg. Chem.* **2007**, *46*, 949.

(3) (a) Voβ, C.; Pattacini, R.; Braunstein, P. *C. R. Chim.* **2012**, *15*, 229. (b) Zank, J.; Schier, A.; Schmidbaur, H. *J. Chem. Soc., Dalton Trans.* **1998**, 323. (c) Fackler, J. P. *Inorg. Chem.* **2002**, *41*, 6959.

(4) (a) Schmidbaur, H. *Gold: Progress in Chemistry, Biochemistry and Technology*; Wiley: Chichester, U.K., 1999. (b) Scherbaum, F.; Grohmann, A.; Huber, B.; Krüger, C.; Schmidbaur, H. *Angew. Chem., Int. Ed. Engl.* **1988**, *27*, 1544. (c) Schmidbaur, H. *Chem. Soc. Rev.* **1995**, *24*, 391.

(5) (a) Muñiz, J.; Wang, C.; Pyykkö, P. *Chem.—Eur. J.* **2011**, *17*, 368. (b) Pyykkö, P. *Chem. Soc. Rev.* **2008**, *37*, 1967. (c) Pyykkö, P. *Angew. Chem., Int. Ed.* **2004**, *43*, 4412. (d) Pyykkö, P.; Li, J.; Runeberg, N. *Chem. Phys. Lett.* **1994**, *218*, 133.

(6) Sculfort, S.; Braunstein, P. *Chem. Soc. Rev.* **2011**, *40*, 2741.

(7) Braunstein, P., Oro, L. A., Raithby, P. R., Eds. *Metal Clusters in Chemistry*; Wiley-VCH: New York, 1999.

(8) (a) Lauher, J. W.; Wald, K. *J. Am. Chem. Soc.* **1981**, *103*, 7648. (b) Braunstein, P.; Rosé, J.; Dusausoy, Y.; Mangeot, J.-P. *C. R. Chim.* **1982**, *294*, 967. (c) Li, X.; Kiran, B.; Wang, L.-S. *J. Phys. Chem. A* **2005**, *109*, 4366.

(9) (a) Hoffmann, R. *Angew. Chem., Int. Ed. Engl.* **1982**, *21*, 711. (b) Mingos, D. M. P. *Gold Bull.* **1984**, *17*, 5. (c) Braunstein, P.; Rosé, J. *Gold Bull.* **1985**, *18*, 17.

(10) (a) van Hal, J. W.; Whitmire, K. H. *Organometallics* **1998**, *17*, 5197. (b) Roland, E.; Fischer, K.; Vahrenkamp, H. *Angew. Chem., Int. Ed. Engl.* **1983**, *22*, 326. (c) Fischer, K.; Deck, W.; Schwarz, M.; Vahrenkamp, H. *Chem. Ber.* **1985**, *118*, 4946. (d) Albano, V. G.; Castellari, C.; Femoni, C.; Iapalucci, M. C.; Longoni, G.; Monari, M.; Rauccio, M.; Zacchini, S. *Inorg. Chim. Acta* **1999**, *291*, 372.

(11) (a) Albano, V. G.; Braga, D.; Martinengo, S. *J. Chem. Soc., Dalton Trans.* **1986**, 981. (b) Albano, V. G.; Braga, D.; Martinengo, S. *J. Chem. Soc., Dalton Trans.* **1981**, 717. (c) Heaton, B. T.; Strona, L.; Martinengo, S. *J. Organomet. Chem.* **1981**, *215*, 415. (d) Martinengo, S.; Strumolo, D.; Chini, P.; Albano, V. G.; Braga, D. *J. Chem. Soc., Dalton Trans.* **1985**, 35. (e) Albano, V. G.; Sansoni, M.; Chini, P.; Martinengo, S. *J. Chem. Soc., Dalton Trans.* **1973**, 651. (f) Albano, V. G.; Chini, P.; Ciani, C.; Sansoni, M.; Martinengo, S. *J. Chem. Soc., Dalton Trans.* **1980**, 163.

(12) (a) Adams, R.; Wu, W. *J. Cluster Sci.* **1991**, *2*, 271. (b) Saha, S.; Zhu, L.; Captain, B. *Inorg. Chem.* **2010**, *49*, 3465. (c) Adams, R. D.; Layland, R.; McBride, K. *Organometallics* **1996**, *15*, 5425. (d) Lange, A.; Meier, W.; Wachter, J.; Zabel, M. *Inorg. Chim. Acta* **2006**, *359*, 1006. (e) Chihara, T.; Yamaaki, H. *J. Organomet. Chem.* **1994**, *473*, 273.

(13) (a) Braga, D.; Grepioni, F.; Dyson, P. J.; Johnson, B. F. G.; Frediani, P.; Bianchi, M.; Piacenti, F. *J. Chem. Soc., Dalton Trans.* **1992**, 2565. (b) Khimyak, T.; Johnson, B. F. G.; Hermans, S.; Bond, A. D. *Dalton Trans.* **2003**, 2651. (c) Johnson, B. F. G.; Lewis, J.; Sankay, S. W.; Wong, K.; McPartlin, M.; Nelson, W. J. H. *J. Organomet. Chem.* **1980**, *191*, 63. (d) Lewis, J.; Morewood, C. A.; Raithny, P. R.; Ramirez de Arellano, M. C. *J. Chem. Soc., Dalton Trans.* **1997**, 3335. (e) Dyson, P. J.; Hearley, A. K.; Johnson, B. F. G.; Khimyak, T.; McIndoe, J. S.; Langride-Smith, P. R. R. *Organometallics* **2001**, *20*, 3970. (f) Beringhelli, T.; D'Alfonso, G.; Molinari, H.; Sironi, A. *J. Chem. Soc., Dalton Trans.* **1992**, 689.

(14) (a) Churchil, M. R.; Wormald, J. *J. Chem. Soc., Dalton Trans.* **1974**, 2410. (b) Koshevoy, I. O.; Haukka, M.; Pakkanen, T. A.; Tunik, S. *Dalton Trans.* **2006**, 5641. (c) Slovokhotov, Yu. L.; Struchkov, Yu. T.; Lopatin, V. E.; Gubin, S. P. *J. Organomet. Chem.* **1984**, *266*, 139. (d) Nakajima, T.; Konomoto, H.; Ogawa, H.; Wakatsuki, Y. *J. Organomet. Chem.* **2007**, *692*, 4886. (e) Tachikawa, M.; Sievert, A. C.; Muetterties, E. L.; Thompson, M. R.; Day, C. S.; Day, V. W. *J. Am. Chem. Soc.* **1980**, *102*, 1725.

(15) (a) Alami, M. K.; Dahan, F.; Mathieu, R. *J. Chem. Soc., Dalton Trans.* **1987**, 1983. (b) Hrijac, J. A.; Holt, E. M.; Shriver, D. F. *Inorg. Chem.* **1987**, *26*, 2943. (c) Kamiguchi, S.; Chihara, T. *J. Cluster Sci.* **2000**, *11*, 483. (d) Jensen, M. P.; Henderson, W.; Johnston, D. H.; Sabat, M.; Shriver, D. F. *J. Organomet. Chem.* **1990**, *394*, 121. (e) Hsu, G.; Wilson, S. R.; Shapley, J. R. *Inorg. Chem.* **1991**, *30*, 3881.

(16) Fumagalli, A.; Martinengo, S.; Albano, V. G.; Braga, D.; Grepioni, F. *J. Chem. Soc., Dalton Trans.* **1989**, 2343.

(17) Reina, R.; Riba, O.; Rossell, O.; Seco, M.; de Montauzon, D.; Pellinghelli, M. A.; Tiripicchio, A.; Font-Bardía, M.; Solans, X. *J. Chem. Soc., Dalton Trans.* **2000**, 4464.

(18) Ceriotti, A.; Longoni, G.; Manassero, M.; Perego, M.; Sansoni, M. *Inorg. Chem.* **1985**, *24*, 117.

(19) Buchowicz, W.; Herbaczyńska, B.; Jerzykiewicz, L. B.; Lis, T.; Pasynkiewiicz, S.; Pietrzykowski, A. *Inorg. Chem.* **2012**, *51*, 8292.

(20) Ceriotti, A.; Piro, G.; Longoni, G.; Manassero, M.; Masciocchi, N.; Sansoni, M. *New J. Chem.* **1988**, *12*, 501.

(21) Bernardi, A.; Femoni, C.; Iapalucci, M. C.; Longoni, G.; Zacchini, S.; Fedi, S.; Zanello, P. *Eur. J. Inorg. Chem.* **2010**, 4831.

(22) Ciabatti, I.; Femoni, C.; Iapalucci, M. C.; Longoni, G.; Zacchini, S.; Fedi, S.; Fabrizi de Biani, F. *Inorg. Chem.* **2012**, *51*, 11753.

(23) (a) Whoolery, A. J.; Dahl, L. F. *J. Am. Chem. Soc.* **1991**, *113*, 6683. (b) Whoolery Johnson, A. J.; Spencer, B.; Dahl, L. F. *Inorg. Chim. Acta* **1994**, *227*, 269.

(24) (a) Cordero, B.; Gómez, V.; Platero-Prats, A. E.; Revés, M.; Echevarría, J.; Cremades, E.; Barragán, F.; Alvarez, S. *Dalton Trans.* **2008**, 2832. (b) Bondi, A. *J. Phys. Chem.* **1964**, *68*, 441.

(25) Wade, K. *J. Chem. Soc. D* **1971**, 792. (b) Wade, K. *Adv. Inorg. Chem. Radiochem.* **1976**, *18*, 1.

(26) Kowala, C.; Swan, J. M. *Aust. J. Chem.* **1966**, *19*, 547.

(27) Keller, E. *SCHAKAL99*; University of Freiburg: Freiburg, Germany, 1999.

(28) Sheldrick, G. M. *SADABS, Program for empirical absorption correction*; University of Göttingen: Göttingen, Germany, 1996.

(29) Sheldrick, G. M. *SHELX97, Program for crystal structure determination*; University of Göttingen: Göttingen, Germany, 1997.

(30) Becke, A. D. *J. Chem. Phys.* **1993**, *98*, 5648.

(31) Grimme, S. *J. Comput. Chem.* **2006**, *27*, 1787.

(32) Frisch, M. J.; Trucks, G. W.; Schlegel, H. B.; Scuseria, G. E.; Robb, M. A.;Cheeseman, J. R.; Scalmani, G.; Barone, V.; Mennucci, B.; Petersson, G. A.; Nakatsuji, H.; Caricato, M.; Li, X.; Hratchian, H. P.; Izmaylov, A. F.; Bloino, J.; Zheng, G.; Sonnenberg, J. L.; Hada, M.; Ehara, M.; Toyota, K.; Fukuda, R.; Hasegawa, J.; Ishida, M.; Nakajima, T.; Honda, Y.; Kitao, O.; Nakai, H.; Vreven, T.; Montgomery, J. A., Jr.; Peralta, J. E.; Ogliaro, F.;Bearpark, M.; Heyd, J. J.; Brothers, E.; Kudin, K. N.; Staroverov, V. N.; Keith, T.; Kobayashi, R.; Normand, J.;Raghavachari, K.; Rendell, A.; Burant, J. C.; Iyengar, S. S.; Tomasi, J.; Cossi, M.; Rega, N.; Millam, J. M.; Klene, M.; Knox, J. E.; Cross, J. B.; Bakken, V.; Adamo, C.; Jaramillo, J.; Gomperts, R.; Stratmann, R. E.; Yazyev, O.; Austin, A. J.; Cammi, R.; Pomelli, C.; Ochterski, J. W.; Martin, R. L.; Morokuma, K.; Zakrzewski, V. G.; Voth, G. A.; Salvador, P.; Dannenberg, J. J.; Dapprich, S.; Daniels, A. D.; Farkas, O.; Foresman, J. B.; Ortiz, J. V.; Cioslowski, J.; Fox, D. J. *Gaussian 09*, revision B.01; Gaussian, Inc.: Wallingford, CT, 2010.

(33) Dolg, M.; Stoll, H.; Preuss, H.; Pitzer, R. M. *J. Phys. Chem.* **1993**, *97*, 5852.